Robotica (2008) volume 26, pp. 109–116. © 2007 Cambridge University Press
doi:10.1017/S0263574707003645 Printed in the United Kingdom

Design aspects and development of humanoid robot THBIP-2

Zeyang Xia†, Li Liu†, Jing Xiong†, Qiang Yi† and Ken Chen†,*

†*Robotics and Automation Laboratory, Department of Precision Instruments and Mechanology, Tsinghua University, Beijing 100084, P. R. China. E-mail: zeyang.xia@ieee.org*

(Received in Final Form: June 4, 2007. First published online: July 5, 2007)

SUMMARY

This is the first publication presenting the minihumanoid robot THBIP-2, the second-generation biped of Tsinghua University. It is 70 cm in height and 18 kg in weight with 24 degrees of freedom. This paper mainly addresses its mechatronics system realization, including the conceptual design, actuation system, sensing system, and control system. In addition, a walking stability controller based on zero moment point criterion and the walking simulation are presented. Finally, experiments validate and confirm the efficiency of the design.

KEYWORDS: Biped walking; Conceptual design; Sensing and actuation; Zero moment point; Gait Planning.

1. Introduction

There has been a rapid and flourishing research progress of humanoid robotics in the last 34 years since the first biped robot Wabot-1 was developed.[1] It has been an interdisciplinary research focus and many institutes around the world have developed various humanoid robots. Some researches concentrate on biped locomotion, some on the humanoid intelligence,[2] and others focus on basic scientific fields, such as new actuation methods.[3] A series of successful humanoid robots has been published, especially the Honda humanoid robots and the Sony humanoid robots, which have achieved complex locomotion patterns and intelligence such as audio and video communication with the human being.[4,5] However, the general research on humanoid robotics is still in the primary period and there are some basic issues to be studied, among which the hardware realization has been a pivotal technology and a bottleneck for the research advancement.

The Robotics and Automation Laboratory of Tsinghua University (RAL-THU) has developed its first-generation humanoid robot THBIP-1 since 2000. It is a human-size 32 degree-of-freedom (DOF) prototype with a height of 174 cm and a weight of 130 kg.[6] It has achieved both stable static walking and slow dynamic walking. Also, it successfully performs climbing upstairs and shadowboxing. THBIP-1 is different from other prototypes because of its special screw-nut-link mechanism utilized in the transmission system at the ankle joint, which affects the locomotion performance with the highest priority among all the joints. This complex mechanism was designed to achieve a high driving torque during some walking phases, given the fact that the curve fluctuation of its transmission matches the fluctuation of the required torque. However, the unfixed transmission ratio also leads to the diversification of the transfer function of the ankle joint, which restricts the joint position tracking ability of the robot.

To resolve this problem, THBIP-2, an infant-size prototype with a different actuation and transmission system, has been developed (see Fig. 1). This paper gives a general introduction of the development of this robot, especially the design aspects and prototype realization. It is organized as follows. Section 2 describes the conceptual design; Sections 3 and 4 present the realization of actuation and sensing system, respectively; Section 5 introduces the control system hardware; Section 6 addresses the general stability controller; Section 7 describes the gait planning method and walking experiments; and Section 8 introduces the conclusions and future work.

* Corresponding author. E-mail: kenchen@tsinghua.edu.cn

2. System Conceptual Design

2.1. *Configuration of degrees of freedom*

The DOF configuration is the primary problem of the mechanical design and mechanics modeling. The locomotion ability is mainly affected by the DOF configuration of the lower limbs. According to the discussion of ref.[7] a leg with seven DOFs, three at the hip, one at the knee, and three at the ankle, will make the robot very adaptive to uneven floors. But considering the complexity of prototype integration design, most humanoid robots are equipped with only six DOFs at one leg. Finally, it is proved that the lack of ankle-yaw DOF does not affect the adaptability of the robot with uneven floors too much.

Figure 2 shows the DOF configuration of THBIP-2. There are totally 24 DOFs, two at each ankle (pitch and roll), one at each knee (pitch), three at each hip (pitch, roll, and yaw), two at each shoulder (pitch and roll), one at each elbow (pitch), one at the wrist (yaw), one at each hand (clamp), and two in the head (pitch and yaw).

An axes intersection design criterion is utilized here. Three axes in each hip intersect at one point and two axes in each ankle intersect at one point. Also, two axes in each shoulder intersect at one point (see Fig. 2). This intersection design decreases the computation complexity of coordinate transformation in the forward kinematics and inverse

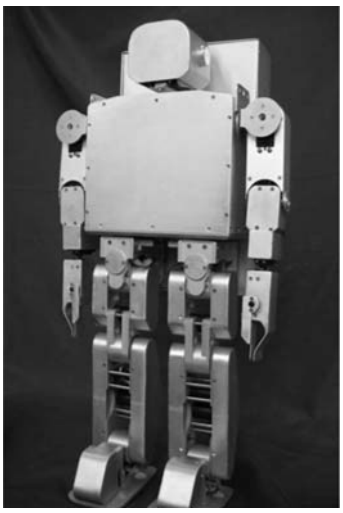

Fig. 1. THBIP-2 prototype.

kinematics calculation.[8] Consequently, it accelerates the gait planning and online gait modification. The intersection design also makes the highly-coupled robot model easier to be decoupled and simplified.

The knees can bend to compensate the unavoidable manufacturing and assembly error to avoid the large offset of the center of gravity (COG) in the sagittal plane when the robot stands vertically.

2.2. *Main physical parameters*

THBIP-2 is 700 mm in height and 18 kg in weight, which makes it convenient to be operated in experiments. Most control components are placed in the thorax and the battery is placed in the backpack. Most mechanical parts are made of aluminum alloy. In order to achieve a successful human-like walking performance, a human-like height and weight distribution of the prototype is strictly considered.[9,10] A comparison of the height/weight distribution between this prototype and the human being is given in Table I. The human body data is from typical Chinese male adults.[11] The numbers in the first/third column are the height/weight proportions of different parts in the whole human body. The numbers in the second/fourth column are the height/weight proportions of different parts in the whole robot prototype. It can be seen that weight/height distribution of THBIP-2 is similar to the male human body, except that the height proportion of the sole is much bigger than the human body because two sets of actuation components are placed there. Other physical parameters are listed in Fig. 3.

Table I. Height/weight distribution comparison.

Ratio	Human height	Robot height	Human weight	Robot weight
Head	0.157	0.149	0.093	0.029
Trunk	0.345	0.388	0.426	0.464
Thigh (×2)	0.252	0.157	0.140	0.064
Calf (×2)	0.220	0.229	0.040	0.071
Sole (×2)	0.026	0.077	0.015	0.036
Upper arm (×2)	*0.185*	*0.157*	0.026	0.043
Forearm (×2)	*0.129*	*0.201*	0.019	0.040

The distance between the two ankle centers is an important parameter. If it is too small, it will limit the motion space of the leg. Specifically, when the robot performs turning-around gait, the soles might collide. If it is too large, the offset between the ground projection of COG and the supporting center during the single-supporting phase will increase. This will decrease the zero moment point (ZMP) stability margin[12,13] and increase the driving load of the roll-DOF of the ankle and the hip joints. After walking simulation and collision analysis, an optimized distance of 130 mm was selected.

Fig. 2. THBIP-2 DOF.

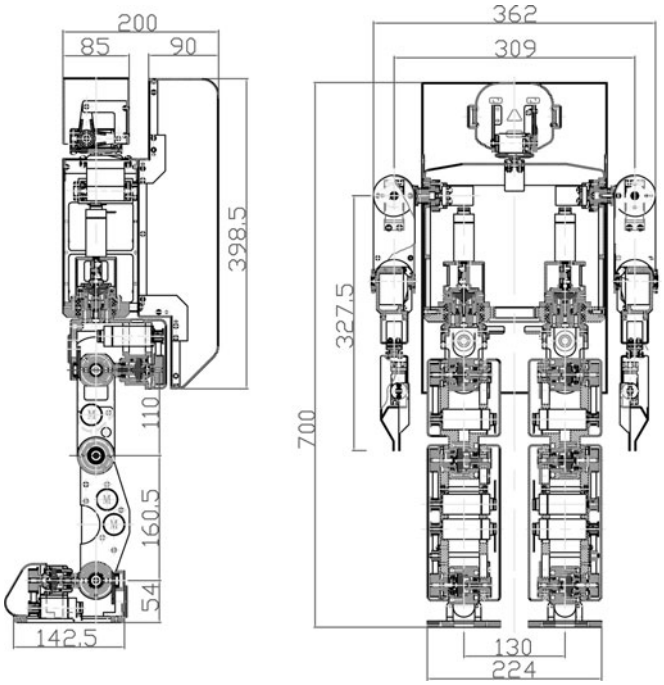

Fig. 3. Physical parameters of THBIP-2 (unit: mm).

Table II. Numerical comparison of different mass distributions.

Torque (Nm)	Ankle roll	Ankle pitch	Knee pitch	Hip pitch	Hip roll	Hip yaw
Case A	3.54	6.22	4.38	1.31	8.54	0.20
Case B	5.11	6.3	4.37	1.27	10.2	0.23

2.3. COG position and mass distribution

The COG position and mass distribution of the robot affect its final dynamic performance.[9] The humanoid-oriented design concept is an important reference for this. According to the dynamic model analysis and comparative simulation experiments, the COG should be over the hip joint center, the intersection point of three-hip DOF. Otherwise, the COG will jump acutely according to the walking rhythm, which leads to big fluctuation of required torque and power driving the key joints of the supporting leg. In addition, the COG should be as low as possible to enhance the stability margin by decreasing the potential overturning moment. Hence, the height of the COG of THBIP-2 is 34.94 cm, while the hip joint height is 32.45 cm.

Some hardware components, e.g., the motor drivers, can be placed in two ways, together in the thorax (Case A) or distributedly near the motors (Case B). In order to achieve an optimal mass distribution, the walking simulations based on the physical models of the previously mentioned two cases were processed. Table II shows the numerical comparison of the required effective torque of DOF of the supporting leg within a single-supporting phase. The second/third row is the required effective torque of the physical models of Case A/B. The contrast is obvious at the ankle-pitch DOF and the hip-roll DOF, which have important effects on the walking performance. Consequently, the integrated mass distribution is preferred in the THBIP-2 prototype.

3. Actuation System

3.1. Analysis of actuation system of humanoid robots

Because most parts of this prototype are made of metal, the weight–height ratio is much bigger than normal human bodies. It is 18 kg to 70 cm for THBIP-2 and 9.6 kg for an infant of the same height.[10] This characteristic severely limits its dynamic performance. New actuators for robots are being explored. The pneumatic artificial muscle has been considered as a potential alternative actuator because of its high power–weight ratio.[3,14] Nonetheless, its current performance on real-time response and repeated accuracy of positioning does not meet the requirements of humanoid walking. That is why nowadays most successfully developed humanoid prototypes are still actuated by motors. In allusion to humanoid robots, especially minihumanoid robots, redundant driving ability is not preferred because it needs driving motors of bigger weights and bigger bulks, which are not permitted by the physical restriction and load restriction. Therefore, motors with too much redundant driving abilities are not preferred.

From another point of view, a humanoid robot can perform different gait patterns with different gait parameters, such as walking forward and backward, turning around, climbing upstairs and downstairs, and jogging. The different patterns with different parameters construct a space, which is nominated as the gait domain. The diverse gait patterns demand different joint actuation abilities. In some situations, the demands fluctuate in a wide range, which makes it impossible for a robot to cover the whole gait domain or most fields of the domain with a fixed set of actuators. In addition, considering the dynamic performance, it is unworthy to pursue a total coverage of the gait domain at the cost of integration of large actuation components.

This characteristic differentiates humanoid robots from industrial robots in design concepts. Herewith, many research groups developed actuator systems themselves, including the motors, motor drivers, and gearings, e.g., the servo actuators of Sony SDR robot.[5] Due to the limited fund and duration of our project, commercial products were selected for THBIP-2.

3.2. Hardware realization of actuation system

The actuation system was designed as follows. The gait planning and inverse dynamics computation with preselected walking parameters was processed to obtain the kinematic and dynamic data of each DOF; then the motors and corresponding transmission mechanisms were selected or designed; these steps with modified model parameters and walking parameters were repeated until an optimization between the coverage of gait domain and mechanical design was achieved.

The computation result of ankle-pitch DOF is given as an example. Figure 4 shows the angle, angular velocity, and angular acceleration of the ankle-pitch DOF during a whole walking gait of 16 s including the initial phase, single-supporting phase, double-supporting phase, and ceasing phase. Figure 5 shows the driving torque and power.

Final reference parameters for the actuation component selection are listed in Table III, where T_{rms} refers to the effective torque. It is computed as:

$$T_{\text{rms}} = \sqrt{\sum_{i=1}^{n} t_i T_i^2 \Big/ \sum_{i=1}^{n} t_i} \tag{1}$$

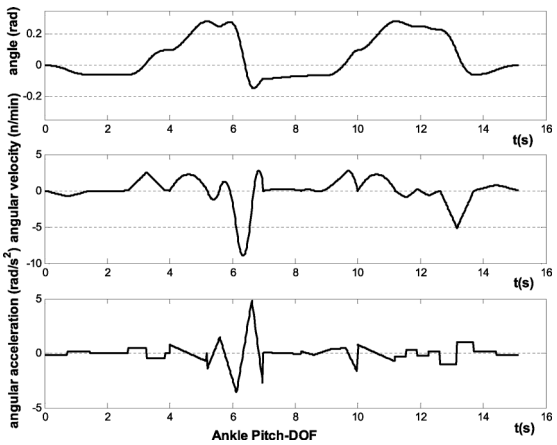

Fig. 4. Kinematics data of a whole walking gait.

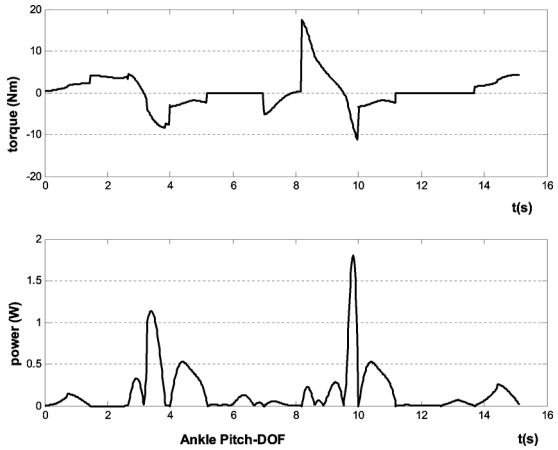

Fig. 5. Dynamics data of a whole walking gait.

Table III. Reference parameters of ankle-pitch DOF.

Item	Value
T_{rms} in single-support phase	7.63 Nm
T_{rms} in double-support phase	3.04 Nm
T_{rms} in a gait period	6.22 Nm
T_{rms} in whole walking period phase	4.19 Nm
Maximal torque in whole gait	16.9 Nm
Maximal angular velocity in whole gait	0.94 rad/s
Maximal angular acceleration in whole gait	5.00 rad/s^2
Maximal power in whole gait	4.43 W

where t_i is the planning interval, which is 0.02 s in our planning, and T_i is the torque in each interval.

Figure 6 shows the final mechanical design of ankle-pitch DOF. Other DOFs were designed likewise and also Faulharber products were selected. Timing belts are used as a reducer because the timing belt combined with harmonic gears is backdrivable, which is advantageous to the joint impact absorption, and it protects the harmonic gear, which is difficult to be disassembled and reassembled if destroyed.

4. Sensing System

4.1. Force sensing system

ZMP stability criterion is utilized in the walking control of THBIP-2.[15] Two six-component force/moment sensors are

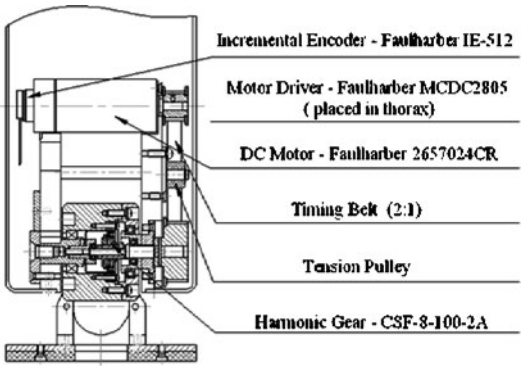

Fig. 6. Hardware realization of ankle-pitch DOF.

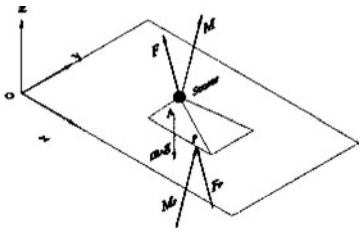

Fig. 7. COP computation model in single-supporting phase.

equipped to measure the ground reaction forces and ZMP position. According to the analysis of ref.[12], the ZMP and Center of Pressure (COP) of locomotion robot superpose on each other during a walking of dynamic balance. Hence, the ZMP position is able to be obtained along with the COP position. Figure 7 shows the COP position computation model in the single-supporting phase.

The COP position in the single-supporting phase, $\mathbf{P}_s$-cop, is computed as:

$$\mathbf{P}_{s\text{-cop}} = \begin{bmatrix} x_{\text{cop}} \\ y_{\text{cop}} \end{bmatrix} = \begin{bmatrix} (x_s\mathbf{F}_z - z_s\mathbf{F}_x - \mathbf{M}_y)/\mathbf{F}_z \\ (y_s\mathbf{F}_z - z_s\mathbf{F}_y + \mathbf{M}_x)/\mathbf{F}_z \end{bmatrix}, \quad (2)$$

where $x_s/y_s/z_s$ denotes the $X/Y/Z$-axis position component of the sensor-measuring center. $\mathbf{F}_x/\mathbf{F}_y/\mathbf{F}_z$ and $\mathbf{M}_x/\mathbf{M}_y$ denote $X/Y/Z$-axis component of ground reaction force and X/Y-axis component of the moment, i.e, the measurement results.

The COP position in the double-supporting phase, $\mathbf{P}_d$-cop, is shown in Fig. 8. It is computed as

$$\mathbf{P}_{d\text{-cop}} = \begin{bmatrix} x_{\text{cop}} \\ y_{\text{cop}} \end{bmatrix} = \begin{bmatrix} (x_1\mathbf{F}_{z1} + x_2\mathbf{F}_{z2})/(\mathbf{F}_{z1} + \mathbf{F}_{z2}) \\ (y_1\mathbf{F}_{z1} + y_2\mathbf{F}_{z2})/(\mathbf{F}_{z1} + \mathbf{F}_{z2}) \end{bmatrix} \quad (3)$$

where x_i/y_i ($i = 1, 2$, denotes foot 1 and foot 2) denotes the X/Y-axis component of COP position of foot i.[15]

4.2. Gesture measurement system

A strapped inertial navigation system is utilized in THBIP-2 to measure the real-time gesture data. The inertial measurement units (IMU) are attached at the upper limb to measure the rotational velocity with respect to the inertial coordinate system and the acceleration with respect to the body-fixed coordinate system by the gyroscope and accelerometers. The output of IMU is processed to obtain

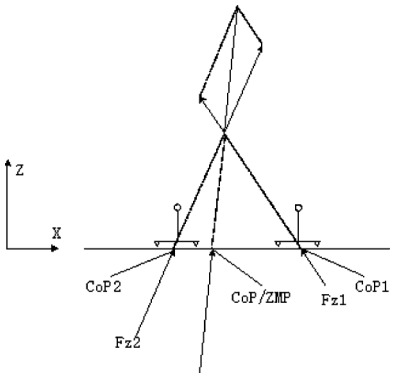

Fig. 8. COP computation model in double-supporting phase.

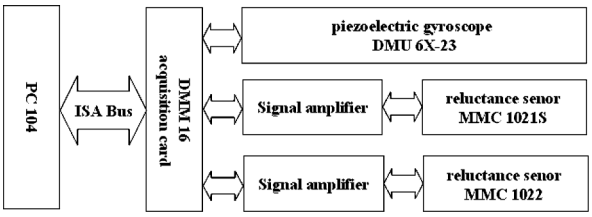

Fig. 9. The gesture measure system of THBIP-2.

the robot gesture and location after error compensation and coordinate transformation. Because of the small distance of the robot locomotion, only the gesture data are the main concern currently. Three accelerometers are equipped in the piezoelectric gyroscope to measure the angular velocity of three directions. A three-dimension reluctance sensor measures the initial gesture. The measurement system is illustrated by Fig. 9.

5. Control System Hardware

Considering the potential extension of sensing systems and the development of more complex algorithms for gait modification and gesture adjustment, a distributed control system based on controller area network (CAN) bus was designed (see Fig. 10).

The main personal computer (PC) performs the tasks of interface management, decision-making, gait planning, and status display. The motion controllers compute the motor control signals, the control voltages of the motors, according to the desired gait data from the main PC and position feedback data from the incremental encoders at the motors. The embedded digital signal processor (DSP) performs the computation of the sensing data. The gait data, joint status, and sensing data are transferred by the CAN bus. Joint status data are directly shared within motion controllers by first-in first-out (FIFO) memories. The TH300 motion controller in Fig. 10 is a small self-developed 3-axes DSP controller with extension slots, which improves the performance of motion synchronization and coordination of multiaxes.

6. Control Algorithm

ZMP theory, the stability criterion for THBIP-2, can be briefly addressed as follows: a legged locomotion machine is able to walk stably if ZMP, the point with respect to which

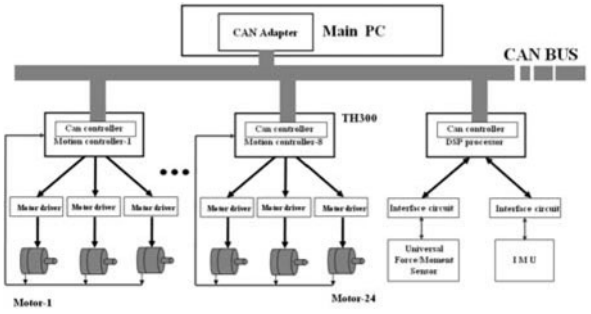

Fig. 10. The CAN-bus-based distributed control system of THBIP-2.

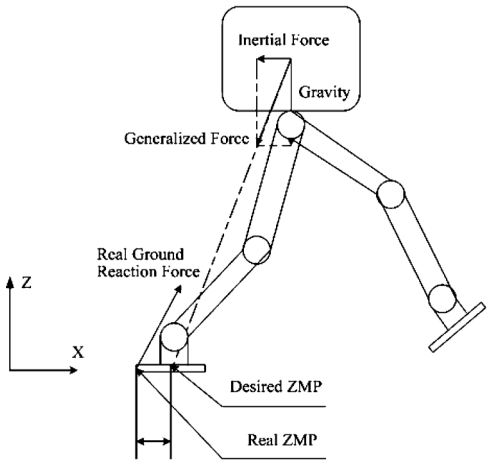

Fig. 11. Dynamic balance model of biped walking.

the moment resulted by the dynamic ground reaction force equals zero, locates within the supporting region, a convex hull of all contact points. It is under the assumption that the ground friction is large enough to ensure that the walking machine does not slip over the ground. Although debates on the availability of ZMP criterion in new situations have been proposed,[12] it is still robustly practical in current static and dynamic walking.

Fig. 11 shows the dynamic balance model of biped walking.[4] The real ZMP is supposed to superpose the desired ZMP during an ideal walking. But, in most cases, overturning moments exist due to the position offset between the real ZMP and the desired ZMP. The 3-axes overturning moment is computed as

$$\begin{bmatrix} \mathbf{T}_{\text{pitch}} \\ \mathbf{T}_{\text{roll}} \\ \mathbf{T}_{\text{yaw}} \end{bmatrix} = \begin{bmatrix} (x_{rzmp} - x_{dzmp})\mathbf{F}_z \\ (\mathrm{y}_{rzmp} - \mathrm{y}_{dzmp})\mathbf{F}_z \\ (x_{rzmp} - x_{dzmp})\mathbf{F}_x + (\mathrm{y}_{rzmp} - \mathrm{y}_{dzmp})\mathbf{F}_y \end{bmatrix} \quad (4)$$

where $\mathbf{T}_{\text{pitch}}/\mathbf{T}_{\text{roll}}/\mathbf{T}_{\text{yaw}}$ denotes $Y/X/Z$-axis component of the overturning moment; x_{rzmp}/Y_{rzmp} denotes X/Y-axis component of the real ZMP position. x_{dzmp}/Y_{dzmp} denotes X/Y-axis component of the desired ZMP position. $\mathbf{F}_x/\mathbf{F}_y/\mathbf{F}_z$ denotes the $X/Y/Z$-axis component of the ground reaction force.

Hence, two balance strategies are utilized, modification of real ZMP position by adjusting the leg posture and modification of the desired ZMP position by adjusting the inertial force. According to the previous analysis, an online gait modification controller was designed (see Fig. 12).

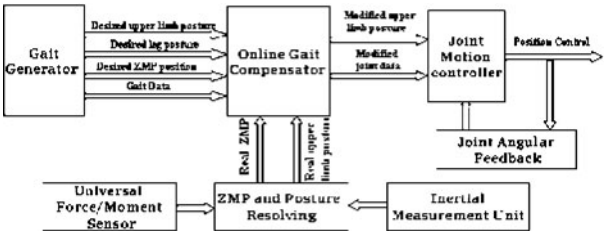

Fig. 12. Diagram of the general stability controller.

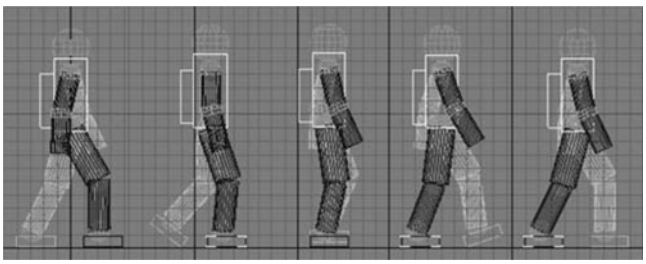

Fig. 13. Walking pattern with nature sole orientation.

Within each gait cycle, the actual gait data, which include the actual ZMP position and real upper limb posture, are computed according to data of the force sensors and the inertial measurement unit (IMU). Then, they are compared with the desired gait data, including the planned joint angles, the planned upper limb posture, and the planned ZMP position, to generate gait modification data.

The computation of inverse Jacobin matrix and decoupling of highly coupled joints is complex when generating the gait modification data. The real-time performance of the modification generator directly affects the final performance of the stability controller. Detailed discussions about the generator will be addressed in our forthcoming publications.

7. Walking Simulation and Experiments

7.1. Gait planning

In order to achieve smooth walking, the robot touches the ground first by the heel of the forward foot and leaves the ground finally by the toe of the latter foot (see Fig. 13). The planning in the sagittal plane is implemented based on the predefinition of the foot trajectory. It is processed as per the following steps:

Step 1: The foot trajectory, including its positions and angles, is planned;

Step 2: The hip trajectory is planned, which must ensure the robot posture to suffice the ZMP stability margin;

Step 3: All other joint trajectories are calculated according to the kinematic constraints.

The planning in the lateral plane is processed likewise and three-order spline interpolation is utilized during the trajectory generation.

7.2. Gait simulation

The gait simulation is processed with walking parameters listed in Table IV. The duration of double-supporting phase is 30%, which is similar to human locomotion.[16] A whole planning cycle includes a single-supporting phase and two double-supporting phases in order to ensure the completeness of the three-order spline interpolation and the smoothness of the phase switch.

Table IV. Gait planning parameters.

Item	Value
Step length	0.16 m
Walking cycle	2 s
Single-supporting phase duration	1.4 s
Double-supporting phase duration	0.6 s
Planning duration	2.6 s

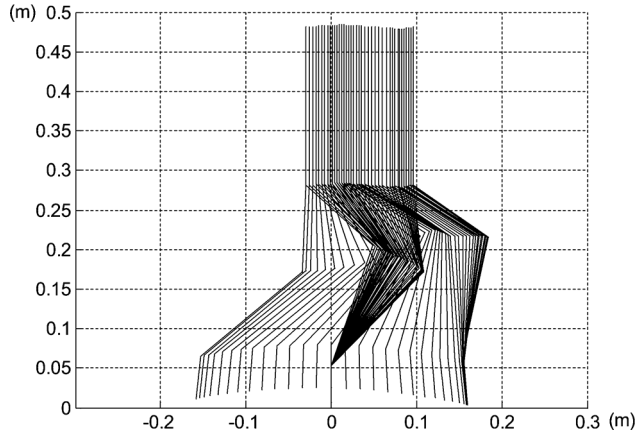

Fig. 14. Stick figure of a walking cycle in the sagittal plane.

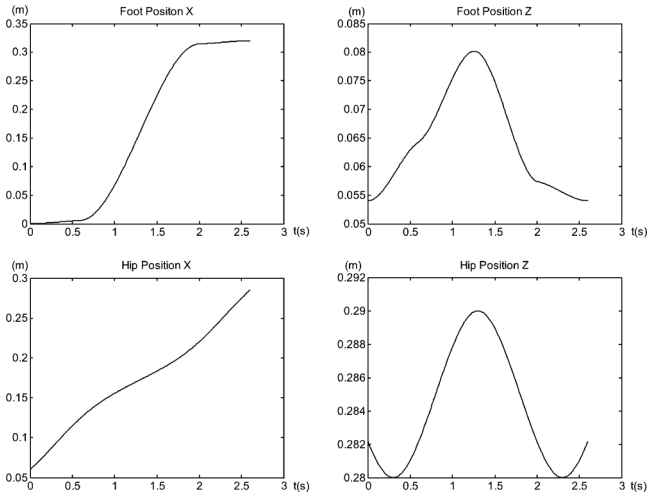

Fig. 15. Foot/hip position in the sagittal plane.

Figure 14 is the stick figure of a walking cycle. The torso trajectory is similar to the sine curve, identical to our analysis of human body locomotion.[17]

The upper row of Figs. 15 and 16 (*left*) show the foot position and orientation during *Step 1*. The bottom row of Fig. 15 shows the hip position during *Step 2*. Fig. 16 (*right*) shows the roll angle of the supporting ankle in the lateral plane. Figure 17 shows the angle, rotation velocity, and rotation acceleration of ankle, knee, and hip joints in the sagittal plane.

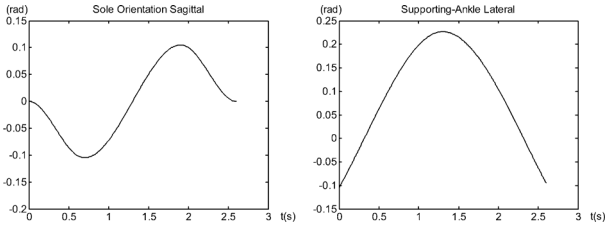

Fig. 16. Foot orientation in the sagittal plane and the angle of the supporting ankle in the lateral plane.

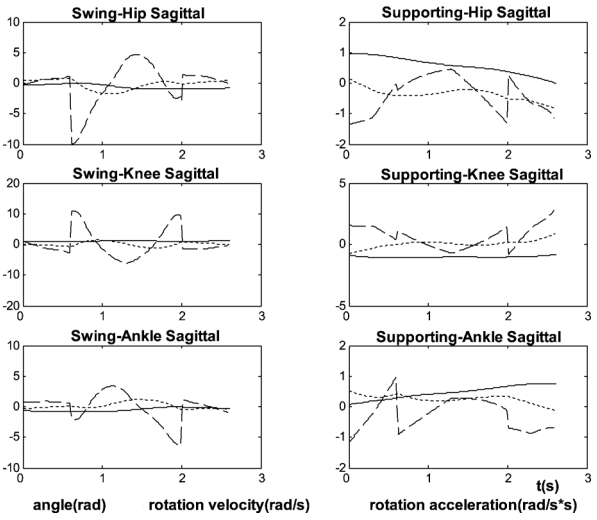

Fig. 17. Kinematic data of ankle/knee/hip in the sagittal plane.

7.3. Experiments

The presented planning algorithm and walking controller have been validated in experiments. A stable walking with a step length of 0.16 m at a velocity of 2 s/step has been achieved. Fig. 18 is a video snapshot of THBIP-2 walking with these parameters. The same planning algorithm and control method have been utilized in THBIP-2 for soccer matches (see Fig. 19).

8. Conclusions and Future Work

Fundamental technologies of developing a humanoid robot, including the conceptual design, hardware realization, control strategy, and gait planning algorithms, are systematically described based on the infant-size humanoid prototype THBIP-2. Some special aspects, such as the mass distribution and the actuation system realization, are presented in detail, which is supposed to provide a reference for ongoing prototype developments. Nowadays, the hardware realization still restricts the general improvement of humanoid robot developments, especially the minihumanoid robots. Improvements of basic research fields, e.g., alternative actuators, will promote the research on humanoid robotics.

Fig. 18. Snapshots of THBIP-2 in walking experiments.

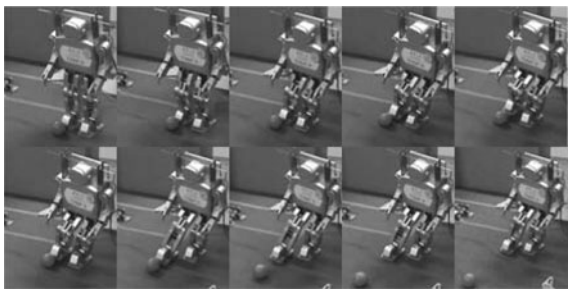

Fig. 19. Snapshots of THBIP-2 in penalty kick.

More copies of THBIP-2 are being developed for multiresearch concerns. Online gait planning and modification, stability control, and motion planning in complex environment would be our future research goals.

Acknowledgments

The authors thank the National Hi-Tech Research and Development Program of China (*863 Plan No.2006AA04Z253*) and National Natural Science Foundation of China (*NSFC No. 50575119*) for sponsoring this research.

References

1. I. Kato, "Development of Wabot-1," **In**: *Biomechanism 2* (The University of Tokyo Press, Tokyo, Japan, 1973) pp. 173–214.
2. R. A. Brooks, et al. "The Cog Project: Building a Humanoid Robot, Computation for Metaphors, Analogy and Agents" **In**: *Springer Lecture Notes in Artificial Intelligence* (C. Nehaniv, ed.), vol. 1562 (Springer-Verlag, Berlin, Germany, 1998).
3. D. G. Caldwell, N. Tsagarakis, D. Badihi and G. A. Medrano-Cerda, "Pneumatic Muscle Actuator Technology: A Lightweight Power System for a Humanoid Robot", *Proceedings of the IEEE International Conference on Robotics and Automation*, Leuven, Belgium (1998) pp. 3035–3058.
4. K. Hirai, M. Hirose, Y. Haikawa and T. Takenaka, "The Development of Honda Humanoid Robot," *Proceedings of the IEEE International Conference on Robotics and Automation*, Leuven, Belgium (May 16–20, 1998) pp. 1321–1326.
5. T. Ishida, Y. Kuroki and J. Yamaguchi, "Mechanical System of a Small Biped Entertainment Robot," *Proceedings of the 2003 IEEE/RSJ International Conference on Intelligent Robot and Systems Las Vegas* Nevada (Oct., 2003) pp. 1129–1134.
6. L. Liu, J. S. Wang, K. Chen, D. C. Yang and J. D. Zhao, "The Research On The Biped Humanoid Robot THBIP-1" *Robot* **24**(3) (2002) pp. 262–267.
7. R. Fred, J. Sias and Y. F. Zheng, "How Many Degrees-of-freedom Does a Biped Need," *Proceedings of the IEEE International Workshop on Intelligent Robtots and System* (1990) pp. 297–302.
8. S. Kajita, H. Hirukawa, K. Yokoi, *et al. Humanoid robots* (Ohmsha, Tokyo, Japan, 2005).
9. J. Hass, J. M. Herrmann and T. Geisel, "Optimal Mass Distribution for Passivity-Based Bipedal Robots," *Int. J. Robot. Res.* **25**, 1087–1098 (2006).
10. V. Zatsiorsky and V. Seluyanov, "The mass and inertia characteristics of the main segments of the human body," *Biomechanics* **8B**, 1152–1159 (1983).
11. *Chinese National Standard GB1000-88, Human Body Data of Chinese Adults*, 1988.
12. M. Vukobratovic, B. Borova and D. Surdilovic, "Zero-Moment Point—Proper Interpretation and New Aplication,"

Proceedings of the IEEE-RAS International Conference on Humanoid Robots (2001) pp. 237–244.
13. Q. Huang, K. Yokoi and S. Kajita, "Planning walking patterns for a biped robot," *IEEE Trans. Robot. Autom.* **17**, 280–289 (2001).
14. F. Daerden and D. Lefeber, "Pneumatic artificial muscles: Actuators for robotics and automation," *Eur. J. Mech. Environ. Eng.* **47**(1), 10C21 (2002).
15. Q. Li, A. Tkanishi and I. Kato, "Development of ZMP measurement system for biped walking robot using universal force-moment sensors," *J. Robot. Soc. Jpn.* **10**(6) 828–833 (1992).
16. V. T. Inman, H. J. Ralston and F. Todd, *Human Walking*, Willams and Wilkins, Baltimore, MD (1981).
17. Z. Y. Xia, K. Chen and L. Liu, "Experimental analysis on humanlocomotion for natural gait planning of humanoid robots," *Robot* **29**(5), 457–462 (in press).